Journal of Ceramic Processing Research. Vol. 23, No. 3, pp. 243~246 (2022)
(Received 3 June 2021, Received in revised form 1 September 2021, Accepted 25 September 2021)
https://doi.org/10.36410/jcpr.2022.23.3.243

J O U R N A L O F
Ceramic Processing Research

Sn-modified $LiNi_{0.9}Co_{0.05}Mn_{0.05}O_2$ cathode with extraordinary electrochemical performances

Chea-Yun Kang and Seung-Hwan Lee*
Department of Materials Science and Engineering, Kangwon National University, Chuncheon 24341, Republic of Korea

We report the synthesis of Sn-modified $LiNi_{0.9}Co_{0.05}Mn_{0.05}O_2$ cathode via a co-precipitation method. The key factor to enhance the electrochemical performances of lithium ion batteries is to suppress the structural reconstruction because of the irreversibility of the H2-H3 phase transition, resulting in rapid performance decay. The as-prepared Sn-modified $LiNi_{0.9}Co_{0.05}Mn_{0.05}O_2$ cathode delivers an initial discharge capacity of 221.4 mAh g^{-1} with a high coulombic efficiency of 88.5 %. Moreover, it shows better polarization of 0.33 V and superior cycle stability of 98.8% after 58 cycles. These values are obviously higher than those of pristine $LiNi_{0.9}Co_{0.05}Mn_{0.05}O_2$ cathode. Therefore, we can believe that Sn-modified $LiNi_{0.9}Co_{0.05}Mn_{0.05}O_2$ cathode is one of the effective way for high-performance cathode material in lithium ion batteries.

Keywords: Sn-modified $LiNi_{0.9}Co_{0.05}Mn_{0.05}O_2$ cathode, structural reconstruction, H2-H3 phase transition, performance decay.

Introduction

Li-ion batteries (LIBs) is widely used for various applications such as electric vehicles (EVs), data centers, uninterruptible power supply (UPS) and hybrid electric vehicles (HEVs) [1]. As well as this, as interest in environment-friendliness increases worldwide, research and applications of sustainable renewable energy (solar, wind and biogas energy) are expanding. Accordingly, interest in energy storage devices (ESDs) that efficiently store and distribute such renewable energy is also explosively increasing. Among the various ESDs (fuel cell, supercapacitor, hybrid supercapacitor and LIBs), LIBs are the most used because of high energy density despite shortcomings in low power density and short lifetime [2].

The cathode is known to determine the electrochemical performance of LIBs. Recently, in order to realize high energy, Ni-rich $LiNiCoMnO_2$ (NCM) has been extensively studied as a promising candidate. However, the cycle stability in Ni-rich NCM is inferior due to unwanted side reactions, H2-H3 phase transition, gas generation, and reduction of Ni^{4+} [3-5]. In order to overcome the shortcomings and maximize the performances of Ni-rich NCM cathode materials, doping, surface modification and morphology control have been reported [6, 7]. Among them, the appropriate amount cation doping is the simplest and easiest way to effectively increase Li ion intercalation, resulting from suppressed phase transformation and voltage decay [8].

*Corresponding author:
Tel : ++82-42-280-2414
E-mail: shlee@dju.kr

Herein, in the present study, we intend to synthesize the Sn-modified $LiNi_{0.9}Co_{0.05}Mn_{0.05}O_2$ cathode with extremely uniform particle size and investigate the electrochemical performances. We reported in a previous paper that Ni-rich NCM doped with 0.05 mol% V had excellent electrochemical performance [3]. Therefore, in this paper, 0.05 mol% Sn was selected as the doping amount. In addition, we discuss the role of the Sn modification in significantly improving electrochemical performances.

Experimental

Spherical Sn-modified $LiNi_{0.9}Co_{0.05}Mn_{0.05}O_2$ powders were prepared by using co-precipitation method. $Ni_{0.9}Co_{0.05}Mn_{0.05}(OH)_2$ precursor was fabricated via appropriate amounts of $NiSO_4 \cdot 6H_2O$, $CoSO_4 \cdot 7H_2O$, $MnSO_4 \cdot H_2O$, Na_2CO_3 and $NH_3 \cdot H_2O$. Precipitating agent was fabricated by NaOH and NH_4OH. Spherical $Ni_{0.8}Co_{0.1}Mn_{0.1}(OH)_2$ was blended with $LiOH \cdot H_2O$ (molar ratio 1.05 : 1) and 0.05 mol% SnO_2. After that, the mixed powders were calcined at 500 °C for 6 h and then sintered at 750 °C for 13 h in tube furnace under atmosphere.

The active materials (96 wt%), polyvinylidene fluoride (PVDF) (2 wt%) and carbon black (Super P, 2 wt%). Subsequently, N-methyl-pyrrolidinone (NMP) solvent was added to prepare slurry. The slurry was coated on Aluminum foil and dried at 120 °C for 12 h. The 2032 coin cells were assembled by Li foil (500 μm in thickness) as an anode in glove box filled with argon gas. 1 M $LiPF_6$ in ethylene carbonate (EC), dimethyl carbonate (DMC) and ethyl methyl carbonate (EMC) (with a volumetric ratio 1 : 1: 1) were adopted as an

electrolyte.

X-ray diffraction (XRD, X'pert MPD DY1219) and field emission scanning electron microscopy (FE-SEM, Hitachi S-4800) were measured to confirm the structural properties (crystallinity and morphology). The electrochemical equipment (TOSCAT-3100, Toyo system) was adopted to measure the charge-discharge tests in the voltage range of 3.0 – 4.3 V. Multi potentiostat (VSP300, Bio-Logic) was used to measure the cyclic voltammetry (CV) in the frequency range of 1 MHz to 10 mHz with 5 mV amplitude.

Results and Discussion

Fig. 1 shows the XRD patterns of Sn-modified and pristine $LiNi_{0.9}Co_{0.05}Mn_{0.05}O_2$ powders. The XRD reflections indicate that both samples are indexed to layered hexagonal α-$NaFeO_2$ structure with a space group R-3m. Both samples have similar XRD peaks, resulting from small amount of Sn introduction. The (003) peak of Sn-modified $LiNi_{0.9}Co_{0.05}Mn_{0.05}O_2$ shifts to lower angle compared to pristine sample via Bragg's law ($n\lambda=2d\sin\theta$) vis larger ionic radius of Sn (0.69 Å) than that of Ni^{2+} (0.56 Å), Co^{3+} (0.54 Å) and Mn^{4+} (0.53 Å). It can be inferred that Sn was effectively doped into the NCM bulk. The significant splitting of the (006)/(102) and (108)/(110) peaks of both samples, indicating excellent crystalline ordering in the hexagonal layered structure [1, 2]. Moreover, both samples have high (003)/(104) intensity ratios, higher than 1.2 (Sn-modified $LiNi_{0.9}Co_{0.05}Mn_{0.05}O_2$: 1.41, pristine $LiNi_{0.9}Co_{0.05}Mn_{0.05}O_2$: 1.29), revealing low cation disordering with lithium ions in 3a site, transition-metal ions in 3b site. This is because the (003)/(104) intensity ratios show the degree of cation mixing in the layered structure. More importantly, the bigger ionic radius of Sn, enabling smooth and rapid electrochemical kinetics [3].

The particle morphologies of both samples are shown in Fig. 2. As expected, the morphology and average particle size of Sn-modified $LiNi_{0.9}Co_{0.05}Mn_{0.05}O_2$ are almost identical to those of pristine $LiNi_{0.9}Co_{0.05}Mn_{0.05}O_2$. Both samples have spherical shape with approximately 11.0 μm, composed of numerous primary particles of about 150 nm diameter. As a result, we can infer that Sn-modification cannot change the microstructures.

As shown in Fig. 3, the initial charge-discharge of both samples are measured in the voltage range of 3.0 – 4.3 V. There are no significant differences in charge-

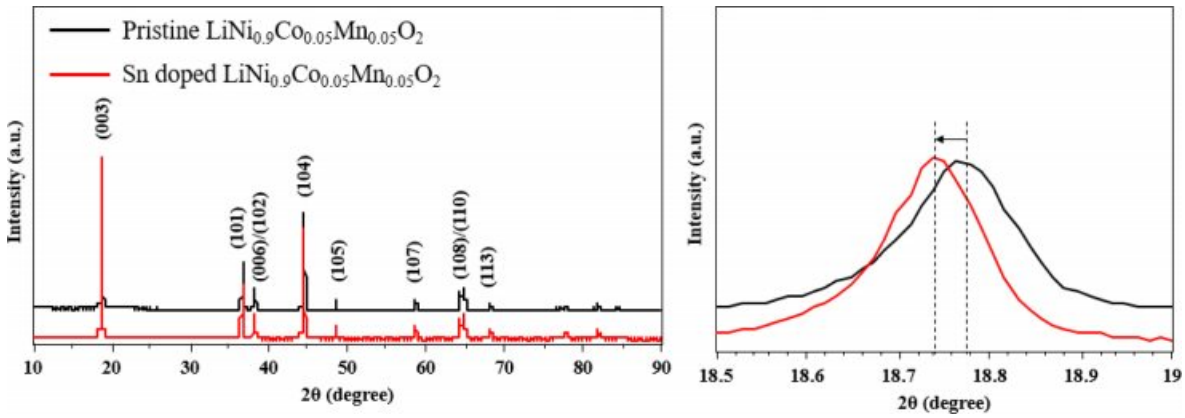

Fig. 1. XRD patterns of Sn doped and pristine $LiNi_{0.9}Co_{0.05}Mn_{0.05}O_2$.

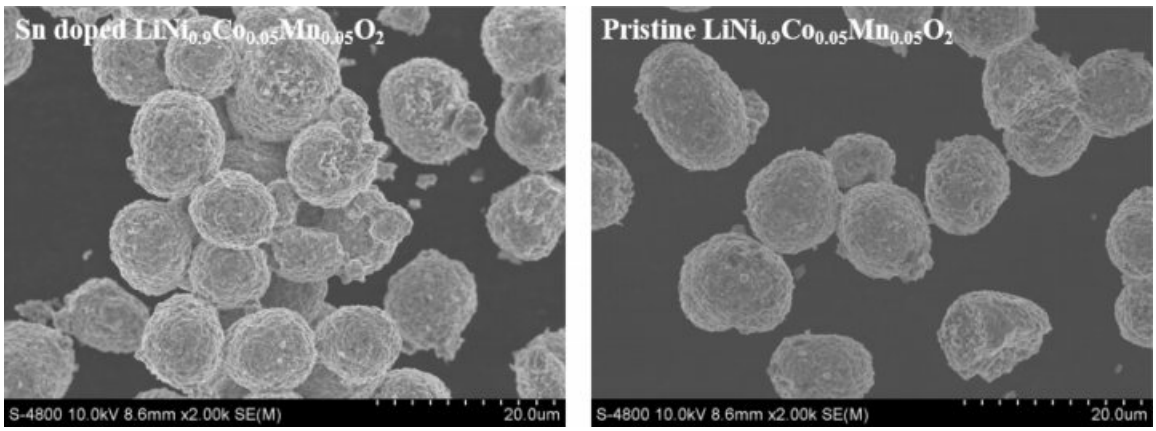

Fig. 2. FESEM images of Sn doped and pristine $LiNi_{0.9}Co_{0.05}Mn_{0.05}O_2$.

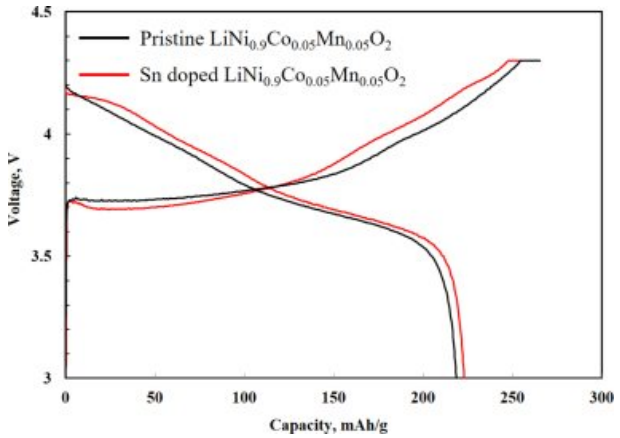

Fig. 3. Initial charge-discharge profiles of Sn doped and pristine $LiNi_{0.9}Co_{0.05}Mn_{0.05}O_2$ at 0.5 C (1 C = 210 mAh g^{-1}).

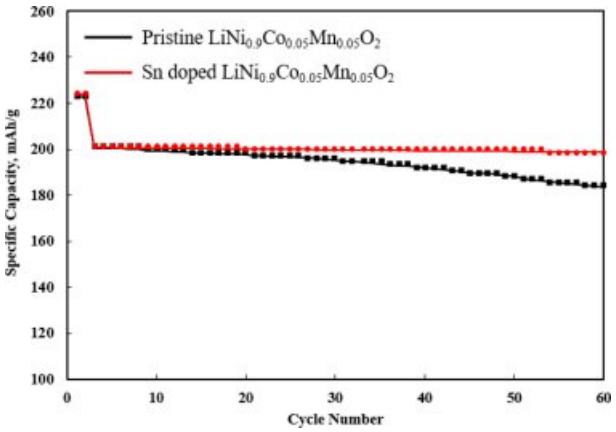

Fig. 5. Cycle performances of Sn doped and pristine $LiNi_{0.9}Co_{0.05}Mn_{0.05}O_2$.

discharge behaviors, which is a usual curves of Ni-rich NCM cathode. The initial discharge capacities of Sn-modified $LiNi_{0.9}Co_{0.05}Mn_{0.05}O_2$ and pristine $LiNi_{0.9}Co_{0.05}Mn_{0.05}O_2$ are 221.4 and 217.8 mAh g^{-1}, respectively. Consequently, it can be confirmed that XX-modification has no significant effect on initial charge-discharge.

The CV curves of Sn-modified $LiNi_{0.9}Co_{0.05}Mn_{0.05}O_2$ and pristine $LiNi_{0.9}Co_{0.05}Mn_{0.05}O_2$ at a scan rate of 0.1 mVs^{-1} in the range of 3.0 – 4.3 V are shown in Fig. 4 to demonstrate the electrochemical phase transition and behavior. Both samples exhibit typical and similar shape of CV curves with several oxidation and reduction peaks. These is closely related to Ni^{2+}/Ni^{4+} and Co^{3+}/Co^{4+} redox couples [4]. These redox peaks are closely related to the phase transformation [5, 6]. There are three pairs of redox peaks, which corresponding to the 3-phase transformation from hexagonal phase to monoclinic phase (H1→M), monoclinic phase to hexagonal phase (M→H2) and hexagonal phase to hexagonal phase (H2→H3) for both samples in the course of the charge/discharge. Among them, the H2-H3 phase transition resultingly causes quick lattice deformation along c-direction, results in electrochemical performance

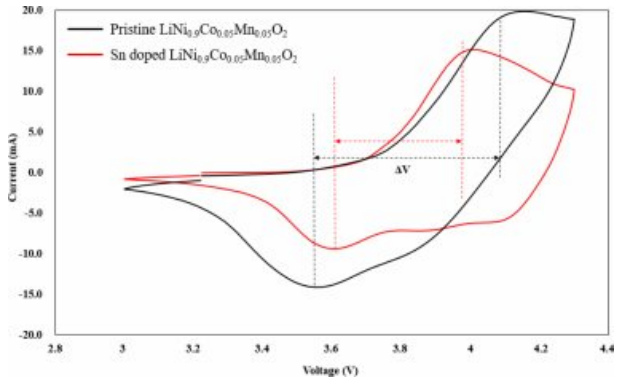

Fig. 4. CV curves of Sn doped and pristine $LiNi_{0.9}Co_{0.05}Mn_{0.05}O_2$ in an EC–DMC-EMC solution at a scan rate of 0.1 mV s^{-1}.

decay [7, 8]. The polarization between redox peaks for Sn-modified $LiNi_{0.9}Co_{0.05}Mn_{0.05}O_2$ is smaller (0.33 V) compared to that of pristine $LiNi_{0.9}Co_{0.05}Mn_{0.05}O_2$ (0.59 V), indicating superior reversible electrochemical performances [9, 10].

The cyclic performance of both samples is measured at 0.5 C between 3.0 V and 4.3 V, as illustrated in Fig. 5. As expected, Sn-modified $LiNi_{0.9}Co_{0.05}Mn_{0.05}O_2$ delivers higher retention than that of pristine $LiNi_{0.9}Co_{0.05}Mn_{0.05}O_2$ under the same conditions. The capacity retentions Sn-modified $LiNi_{0.9}Co_{0.05}Mn_{0.05}O_2$ and pristine $LiNi_{0.9}Co_{0.05}Mn_{0.05}O_2$ are 98.8% and 92.1%, respectively after 58 cycles. These results are due to the superior interfacial stability on the surface of Sn-modified $LiNi_{0.9}Co_{0.05}Mn_{0.05}O_2$ and, leading to the enhanced structural stability with less Ni dissolution [11, 12]. It can be assumed that the pristine $LiNi_{0.9}Co_{0.05}Mn_{0.05}O_2$ has a micro-cracking, resulting from the stress from volume expansion and shrinkage after cycling, which confirms our previous result [13, 14]. The secondary aggregate structure in pristine $LiNi_{0.9}Co_{0.05}Mn_{0.05}O_2$ practices highly anisotropic volume change in lattice dimension, which generate the cracking at the grain boundaries. It ultimately increase the contact area of pristine $LiNi_{0.9}Co_{0.05}Mn_{0.05}O_2$ and then cause more side reactions between cathode and electrolyte during long term cycling. Consequently, these phenomena disturb electronic and ionic transport thereby degrading electrochemical performances [15].

Conclusion

In this study, we design and successfully synthesize the Sn-modified $LiNi_{0.9}Co_{0.05}Mn_{0.05}O_2$ for high-energy LIBs and investigate the electrochemical performances through phase transition. The Sn-modified $LiNi_{0.9}Co_{0.05}Mn_{0.05}O_2$ enables smooth and rapid lithium ion transfer. Moreover, the Sn modification can maintain the original layered structure via stable surface chemistry. As a result, Sn-modified $LiNi_{0.9}Co_{0.05}Mn_{0.05}O_2$ can realize not only higher initial discharge capacity but also

excellent long-term cycle performance by effectively suppressing H2-H3 phase transition. Therefore, we can conclude that Sn-modification can be one of the way for next-generation cathode materials.

Acknowledgement

This work was supported by the National Research Foundation of Korea (NRF) grant funded by the Korea government (MSIT) (No. 2021R1F1A1055979). Following are results of a study on the "Leaders in INdustry-university Cooperation +" Project, supported by the Ministry of Education and National Research Foundation of Korea.

References

1. Y. K. Li, W. X. Wang, C. Wu, and J. Yang, Trans. Electr. Electron. Mater. 23[1] (2022) 64-71.
2. Z. Chen, J. Wang, D. Chao, T. Baikie, L. Bai, S. Chen, Y. Zhao, T.C. Sum, J. Lin, Z. Shen, Scientific Reports 6 (2016) 25771.
3. S.J. Sim, S.H. Lee, B.S. Jin, H.S. Kim, Scientific Reports 9 (2019) 8952.
4. S.J. Sim, S.H. Lee, B.S. Jin, H.S. Kim, Scientific reports 10 (2020) 11114.
5. S.H. Lee, B.S. Jin, H.S. Kim, Scientific reports 9 (2019) 17541.
6. T. Sattar, S.H. Lee, B.S. Jin, H.S. Kim, Scientific reports 10 (2020) 8562.
7. S.J. Jo, D.Y. Hwang, S.H. Lee, ACS Appl. Energy Mater. 4 (2021) 3693-3700.
8. D.Y. Hwang, S.J. Sim, B.S. Jin, H.S. Kim, S.H. Lee, ACS Appl. Energy Mater. 4 (2021) 1743-1751.
9. Y. Xia, J. Zheng, C. Wang, M. Gu, Nano Energy 49 (2018) 434-452.
10. S.H. Lee, K.Y. Kim, J.R. Yoon, NPG Asia Materials, 12 (2020) 28.
11. J. Zahnow, T. Bernges, A. Wagner, N. Bohn, J.R. Binder, W.G. Zeier, M.T. Elm, J. Janek, ACS Appl. Energy Mater. 4 (2021) 1335-1345.
12. Y. Zhou, Z. Hu, Y. Huang, Y. Wu, Z. Hong, J. Alloys. Comp. 888 (2021) 161584.
13. A. Habibi, M. Jalaly, R. Rahmanifard, M. Ghorbanzadeh, J. Alloys. Comp. 834 (2020) 155014
14. Y. Zhend, N. Xu, S. Chen, Y. Liao, G. Zhong, Z. Zhang, Y. Yang, ACS Appl. Energy Mater. 3 (2020) 2837-2845.
15. P. Vanaphuti, S. Bong, L. Ma, S. Ehrlich, Y. Wang, ACS Appl. Energy Mater. 3 (2020) 4852-4859.